SOX9 Transcriptionally Regulates mTOR-Induced Proliferation of Basal Cell Carcinomas

Arianna L. Kim[1,3], Jung Ho Back[1,3], Sandeep C. Chaudhary[2], Yucui Zhu[1], Mohammad Athar[2] and David R. Bickers[1]

Currently available smoothened targeted therapies in patients with basal cell nevus syndrome are associated with substantial tumor recurrence and clinical resistance. Strategies bypassing smoothened and/or identifying additional downstream components of the Hedgehog pathway could provide novel antitumor targets with a better therapeutic index. Sry-related high mobility group box 9 (SOX9) is a Hedgehog/glioma-associated oncogene homolog-regulated transcription factor known to be overexpressed in basal cell carcinomas (BCCs). A sequence motif search for SOX9-responsive elements identified three motifs in the promoter region of mammalian target of rapamycin (mTOR). In murine BCC cells, SOX9 occupies the mTOR promoter and induces its transcriptional activity. Short hairpin RNA (shRNA)-mediated knockdown of *SOX9*, as well as smoothened inhibition by itraconazole and vismodegib, reduces mTOR expression and the phosphorylation of known downstream mTOR targets. These effects culminate in diminishing the proliferative capacity of BCC cells, demonstrating a direct mechanistic link between the Hedgehog and mTOR pathways capable of driving BCC growth. Furthermore, rapamycin, a pharmacologic mTOR inhibitor, suppressed the growth of UV-induced BCCs in Ptch1$^{+/-}$/SKH-1 mice, a model that closely mimics the accelerated BCC growth pattern of patients with basal cell nevus syndrome. Our data demonstrate that Hedgehog signaling converges on mTOR via SOX9, and highlight the SOX9-mTOR axis as a viable additional target downstream of smoothened that could enhance tumor elimination in patients with BCC.

Journal of Investigative Dermatology (2018) **138,** 1716–1725; doi:10.1016/j.jid.2018.01.040

INTRODUCTION

Aberrant Hedgehog (Hh) signaling drives numerous types of human malignancies, including basal cell carcinoma (BCC) (Athar et al., 2014). Signaling activation occurs when a secreted ligand (e.g., SHH) binds to the transmembrane receptor patched 1 (PTCH1). Unliganded PTCH1 blocks Hh signaling by repressing the activity of a second transmembrane receptor, smoothened (SMO) (Kar et al., 2012). The binding of ligand to PTCH1 relieves SMO repression, triggering SMO translocation to the primary cilium, where it activates the glioma-associated oncogene homolog family of transcription factors (GLI1-3). GLI then translocates to the nucleus and promotes the transcription of target genes, involved in cell proliferation, metastasis, survival, and stemness, including *PTCH1*, *GLI1*, *CCND1* (cyclin D1), and bone morphogenic proteins (Briscoe and Therond, 2013; Robbins et al., 2012).

Alterations in Hh regulatory components (i.e., loss-of-function mutations in *PTCH1*, gain-of-function mutations in *SMO*, missense mutations in *GLI1* and *GLI3*, concurrent copy number changes in *SUFU* and *GLI2*) drive Hh signaling that is crucial for BCC growth (Athar et al., 2014; Atwood et al., 2012). In addition, germline mutations in the *PTCH* allele are responsible for basal cell nevus syndrome (BCNS)/Gorlin syndrome, an autosomal dominant condition (Gorlin, 1987; Hahn et al., 1996; Johnson et al., 1996). Patients with BCNS typically develop large numbers of BCCs and are at substantially increased risk for other types of Hh-driven neoplasms, including medulloblastomas and rhabdomyosarcomas. Therapies targeted at components of the Hh pathway, including the SMO inhibitor vismodegib, have shown remarkable therapeutic efficacy in patients with BCNS (Tang et al., 2012). However, subsequent studies have revealed significant tumor recurrence and acquired resistance, primarily through secondary mutations in *SMO* (i.e., D473G, D473Y, Q477E, and G497W) that impair drug binding and/or reactivate the Hh pathway (Pricl et al., 2015; Sharpe et al., 2015). Moreover, the presence of *SMO* variants with diminished or absent drug binding in untreated BCCs suggests that some tumors may be intrinsically refractory to currently available SMO inhibitors (Atwood et al., 2015), underscoring

[1]Department of Dermatology, Columbia University Medical Center, New York, New York, USA; and [2]Department of Dermatology, University of Alabama at Birmingham, Birmingham, Alabama, USA

[3]These authors contributed equally to this work.

Correspondence: Arianna L. Kim, Department of Dermatology, Columbia University Medical Center, 1150 St. Nicholas Ave 318A, New York, New York 10032, USA. E-mail: ak309@cumc.columbia.edu

Abbreviations: 4E-BP, 4E binding protein; AKT, v-akt murine thymoma viral oncogene homolog; BCC, basal cell carcinoma; BCNS, basal cell nevus syndrome; CCND1, cyclin D1; GLI, glioma-associated oncogene homolog; HEK, human embryonic kidney; ITRA, itraconazole; mTOR, mammalian target of rapamycin; PTCH1, patched 1; S6K, S6 kinase; SCC, squamous cell carcinoma; SOX, Sry-related high mobility group box 9; TSS, transcription start site

Received 16 November 2017; revised 17 January 2018; accepted 28 January 2018; accepted manuscript published online 14 March 2018; corrected proof published online 18 May 2018

the need for alternative treatment strategies bypassing SMO and/or identification of additional targets amenable to therapeutic intervention.

Recent data highlight involvement of multiple tumor driver pathways in BCC pathogenesis and suggest that their cooperative interactions with the Hh pathway may likely modulate the downstream Hh signaling network and provide novel therapeutic targets. In this regard, we have recently demonstrated that v-akt murine thymoma viral oncogene homolog (AKT), a serine/threonine protein kinase belonging to the phosphatidylinositol 3-kinase/AKT/mammalian target of rapamycin (PI3K/AKT/mTOR) pathway, is required for BCC tumorigenesis, and that it acts downstream of the Hh pathway (Kim et al., 2016) suggesting a crosstalk between Hh signaling and the phosphatidylinositol 3/AKT/mTOR pathway. In this study, we demonstrate that mTOR is a direct transcriptional target of SOX9, an Sry-like high mobility group box transcription factor that is transcriptionally regulated by GLI (Bien-Willner et al., 2007; Eberl et al., 2012; Vidal et al., 2008). We further show that depletion of SOX9 attenuates mTOR signaling and the proliferative capacity of murine BCC cells, and that the pharmacologic inhibition of mTOR suppresses UV-induced BCC tumorigenesis in Ptch1$^{+/-}$/SKH-1 mice, a model that closely mimics the spontaneous and accelerated growth pattern of BCCs in patients with BCNS.

RESULTS

SOX9 is elevated in BCC

We used Ptch1$^{+/-}$/SKH-1 hairless mice to explore the role of SOX9 in BCC growth. Unlike other relevant murine models, which develop BCCs or squamous cell carcinomas (SCCs) but not both, Ptch1$^{+/-}$/SKH-1 mice (hereafter referred to as Ptch1$^{+/-}$) develop both tumor types in response to chronic UV exposure, allowing us to decipher the molecular determinants underlying the growth of these tumors in the same genetic background (Chaudhary et al., 2015). We first assessed SOX9 levels in BCCs and SCCs developed in UV-irradiated Ptch1$^{+/-}$ mice. SOX9 levels were strongly elevated in BCCs compared with that observed in nontumor-bearing stroma regions (Figure 1a and c). The majority of cells in BCCs showed elevated SOX9 expression, whereas its expression was limited to only a few cells in SCCs (Figure 1a). Consistent with murine BCCs, SOX9-positive staining was also confined to tumor cells in the human BCC biopsies (Figure 1b and d) and was mostly absent in nontumor-bearing adjacent tissues in both murine and human BCCs, detectable only in patches in the basal cell layers (Figure 1a and b, arrows). The majority of SCCs (23 of a total of 32 human SCCs represented in a tissue microarray) lacked SOX9 staining (Figure 1e). The remaining SCCs showed some degree of SOX9 positivity; however, more than one-half of these had staining in less than 10% of the tumor areas—with the exception of a few cases of invasive and recurrent SCCs (3/4), which showed intense staining comparable to that observed in BCCs (Figure 1e). Although the relevance of SOX9 to SCC growth requires further validation, our data indicate that SOX9 is predominantly augmented in BCCs.

SOX9 knockdown suppresses the proliferative capacity of murine BCC cells

ASZ001 cells, derived from BCCs induced in UV-irradiated Ptch1$^{+/-}$/C57BL6 mice, provide a relevant in vitro BCC model, as they display a cellular morphology virtually identical to that occurring in human BCCs, express typical BCC markers, and are sensitive to SMO inhibition (Aszterbaum et al., 1998; So et al., 2006). The remaining wild-type *Ptch1* allele is also lost in these cells, thus mimicking the germline mutations that occur in patients with BCNS (So et al., 2006). We confirmed SOX9 expression in ASZ001 cells and assessed the effects of SOX9 knockdown using three different shRNA constructs (shSOX9-1, -2, -3). All three shSOX9 constructs effectively abolished SOX9 and led to concurrent decreases in the cell proliferation markers proliferating cell nuclear antigen and cyclin D1 that we previously showed to be elevated in BCCs (Chaudhary et al., 2015) (Figure 2a). We further show that SOX9 knockdown significantly diminished (threefold) 5-ethynyl-2′-deoxyuridine incorporation—indicative of cells in the S phase—in ASZ001 cells (Figure 2b and c). These data demonstrate that SOX9 functions to promote the growth of BCC cells.

mTOR is a transcriptional target of SOX9

Our recent study showed that AKT activation is required for the growth of BCCs in Ptch1$^{+/-}$ mice (Kim et al., 2016). While exploring a mechanistic link between the AKT and Hh pathways, we observed that SOX9 and mTOR protein and mRNA levels were markedly increased in Ptch1-deficient primary keratinocytes isolated from newborn Ptch1$^{+/-}$ mice compared with wild-type Ptch1$^{+/+}$ keratinocytes, showing 1.7-fold and 1.8-fold increases in SOX9 and mTOR mRNA levels, respectively (Figure 3a and b). The increased mTOR expression concurrent with SOX9 suggested that mTOR may be regulated by Hh transcriptional factors. We carried out a sequence motif search for the canonical consensus motifs for GLI and SOX9 and found that the consensus GLI-binding sequence present in many direct GLI target genes (Hui and Angers, 2011; Kinzler and Vogelstein, 1990) was not present in the mTOR promoter. Instead, at least three SOX9-binding motifs ([A/T][A/T]CAA[A/T]G) (Kadaja et al., 2014) were present in the promoter region of mTOR (Figure 3c). Electrophoretic mobility gel shift assays demonstrated the binding capacity of nuclear extracts prepared from ASZ001 cells to the −3039 fragment, which was substantially reduced after the shRNA-mediated knockdown of SOX9 (Figure 3d). Chromatin immunoprecipitation verified precipitation of the −3039 and −8283 fragments in ASZ001 cells (Figure 3e). The binding capacity of the −14096 fragment was weaker than the other two (data not shown) and thus excluded from further analyses. To determine the functionality of the SOX9 binding sequences in transcriptional regulation of mTOR, we performed a luciferase reporter assay in ASZ001 cells. Modest reporter activities were detected in cells transduced with either vector alone (pGL3-Basic) or the +1 kb fragment (+1 kb from the transcription start site (TSS); Figure 3f, +1). The addition of −1 kb upstream region led to threefold increases in the reporter activity (Figure 3f, −1/+1), indicating active mTOR transcription in ASZ001 cells. The addition of the −3039 fragment, cloned upstream (5′) of the −1/+1

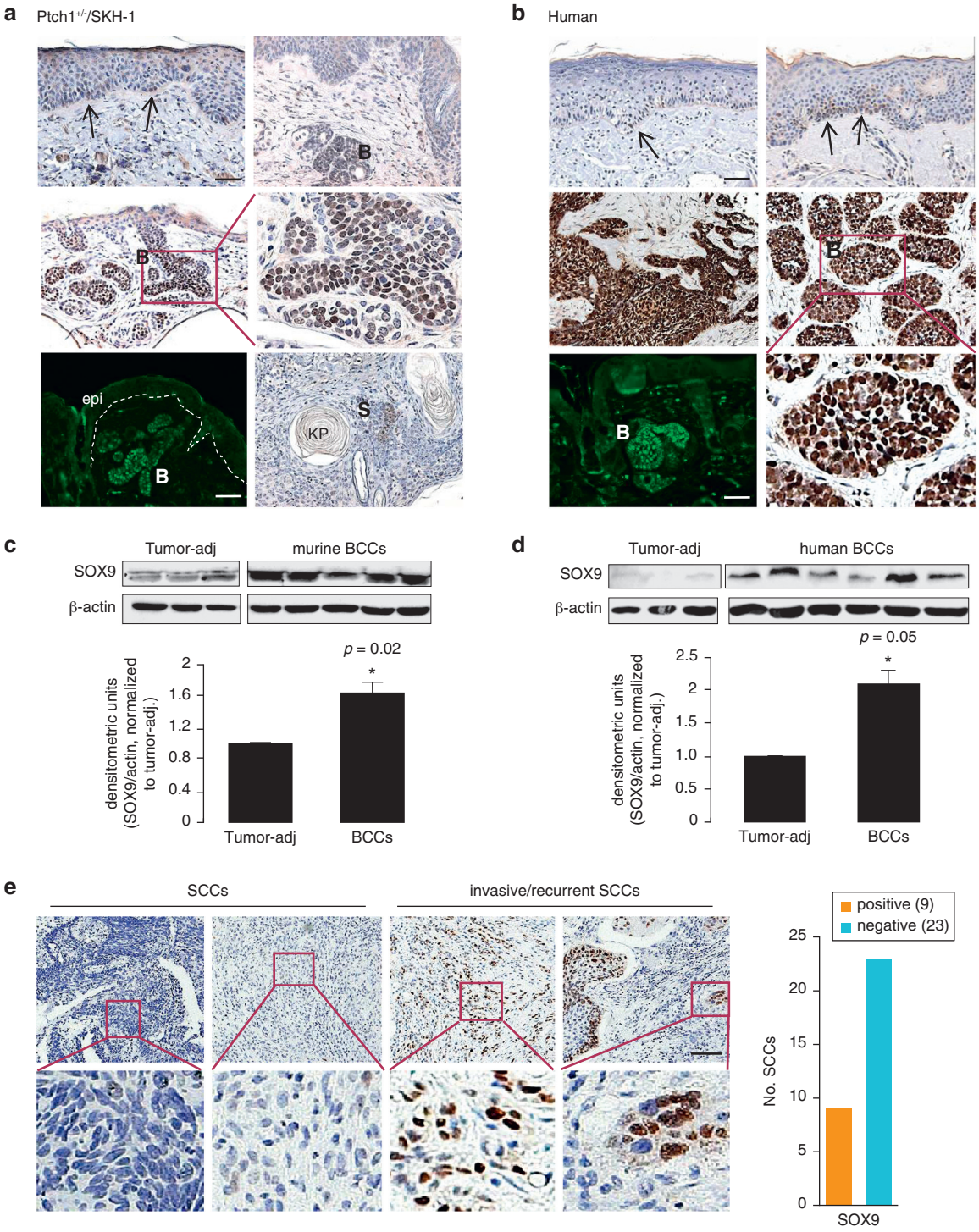

Figure 1. SOX9 is predominantly overexpressed in murine and human BCCs. (**a, b**) Immunohistochemical and immunofluorescent detection of SOX9 in UV-induced murine BCCs and SCCs in Ptch1$^{+/-}$ mice (**a**), and human sporadic BCCs (**b**). Representative images are shown. Arrows, positive staining for SOX9; KP, keratin pearl; B, BCC; S, SCC. Scale bars = 50 μm. (**c, d**) SOX9 levels in UV-induced murine (**c**) and human (**d**) BCCs, compared with tumor-adjacent skin, detected by western blotting. Histograms represent densitometric scanning of western blots. β-Actin, an internal loading control. Twenty micrograms of protein per lane. (**e**) Immunohistochemical assessment of SOX9 in human cutaneous SCC tissue microarray (n = 32). Histogram: the number of SCCs showing positive or negative staining for SOX9. SCC with SOX9 staining in >10% of tumor cells within the tumor areas was considered positive. Scale bar = 100 μm. BCC, basal cell carcinoma; PTCH1, patched 1; SCC, squamous cell carcinoma; SOX9, Sry-related high mobility group box 9.

region, further enhanced the reporter activity, showing a 4.1-fold increase compared with the vector alone (Figure 3f, −3039). The −8283 fragment also showed substantial increases compared with the vector alone, although this is a modest increase as compared with the −1/+1 fragment (Figure 3f, −8283). These results demonstrate that the −3039 region is indeed functional in ASZ001 cells and provide evidence for a mechanistic link between SOX9 and mTOR.

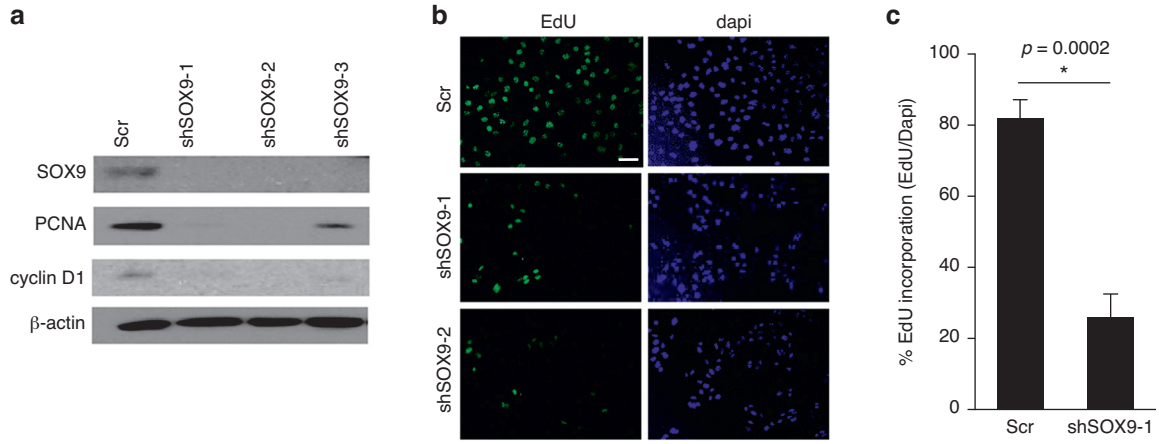

Figure 2. SOX9 knockdown suppresses the proliferation of ASZ001 murine basal cell carcinoma cells. (**a**) PCNA and cyclin D1 levels in ASZ001 cells stably transduced with three different SOX9-specific shRNAs (shSOX9-1, -2, -3) or scrambled shRNA (Scr), assessed by western blotting. β-Actin was used as an internal control. Twenty micrograms of protein per lane. (**b**) EdU incorporation assay in ASZ001 cells transduced with Scr, shSOX9-1, or shSOX9-2. Green, EdU; blue, DAPI. Scale bar = 100 μm. (**c**) Quantitation of EdU-labeled ASZ001 cells transduced with Scr or shSOX9-1. Data represent the mean ± standard deviation of three independent experiments. EdU, 5-ethynyl-2′-deoxyuridine; PCNA, proliferating cell nuclear antigen; shRNA, short hairpin RNA; SOX9, Sry-related high mobility group box 9.

mTOR is known to promote cell proliferation and growth through phosphorylation of numerous substrates, including the eukaryotic initiation factor 4E-binding proteins (4E-BPs) and the ribosomal S6 kinases (S6Ks) 1 and 2. Cyclin D1 is also regulated to a limited degree by mTOR-dependent translation (Saxton and Sabatini, 2017). We show that mTOR colocalizes with SOX9 in ASZ001 cells (Figure 3g), and that shRNA-mediated SOX9 knockdown reduced the expression of mTOR (Figure 3g and h) and cyclin D1, as well as the phosphorylation of p-4E-BP1 and p-p70S6K (Figure 3h, lanes 1 vs. 3) to a level comparable to that seen after treatment with the mTOR inhibitor rapamycin (Figure 3h, lanes 2 vs. 3). SOX9-dependent mTOR regulation was further demonstrated using human embryonic kidney (HEK293) cells and HEK293T, a line derived from HEK293 that expresses a mutant version of the SV40 large T antigen (Fonseca et al., 2011). mTOR is expressed at low levels in HEK293 cells, whereas it is elevated in HEK293T cells. Similar to our findings in ASZ001 cells, SOX9 knockdown resulted in decreased mTOR levels in HEK293T cells (Figure 3i). Conversely, SOX9 overexpression in HEK293 cells substantially augmented mTOR expression (Figure 3j). Taken together, our data indicate that SOX9 participates in regulating mTOR signaling in ASZ001 cells and that the SOX9-mTOR axis is also operative in HEK293 cells.

Hh signaling converges on the mTOR pathway via SOX9

To determine the relevance of the SOX9-mTOR axis in the context of the Hh pathway, we assessed SOX9 and mTOR signaling in ASZ001 cells treated with the SMO inhibitor itraconazole (ITRA), an FDA-approved azole antifungal drug recently shown to be a potent and specific inhibitor of Hh signaling (Kim et al., 2010). The treatment of ASZ001 cells with ITRA dose-dependently attenuated SOX9 and mTOR levels and the phosphorylation of p70S6K in ASZ001 cells (Figure 4a), the levels of which were restored by SOX9 overexpression (Figure 4b). In addition, both ITRA (1−30 μM) and vismodegib (IC50 of 40 μM in ASZ001 cells) substantially reduced mTOR mRNA levels, whereas the thymidylate synthase inhibitor 5-fluorouracil, which is FDA-approved to treat superficial BCCs, had no significant effect on mTOR mRNA levels (shown for 40 μM) (Figure 4c). A concurrent decrease in SOX9 and mTOR levels was also observed in BCCs harvested from UV-irradiated Ptch1$^{+/-}$ mice treated with orally administered ITRA (100 mg/kg, twice daily, 24 days) (Figure 4d and e). We further show that mTOR is overexpressed in a substantial fraction of human BCCs (Figure 4f), and mTOR-positive cells were detectable across all three clinical BCC subtypes (i.e., nodular, morpheaform, and superficial BCCs) (Figure 4g, showing nodular and morpheic BCCs). Taken together, our data indicate that the SOX9-mTOR axis could be a viable alternative therapeutic target downstream of SMO.

mTOR inhibitor rapamycin suppresses UV-induced growth of BCCs in Ptch1$^{+/-}$ mice

To directly test the in vivo feasibility of targeting mTOR in BCCs, we assessed the ability of the mTOR inhibitor rapamycin to inhibit UV-induced BCC growth in Ptch1$^{+/-}$ mice. Sixty minutes before UV irradiation (180 mJ/cm^2, twice a week), mice received either rapamycin (40 μg/mouse in 100 μl phosphate buffered saline, intraperitoneally, n = 20), or a vehicle control (n = 20) for 36 weeks. Rapamycin treatment substantially reduced the total BCC tumor burden, resulting in 3-fold and 6.6-fold decreases in tumor number and size, respectively (Figure 5a and b). At week 36, both the number and size of microscopic BCCs were significantly reduced (4-fold and 3.6-fold, respectively) (Figure 5c and d), which correlated with decreases in mTOR as well as its substrates (4EBP, p70S6K) and their phosphorylated counterparts (Figure 5e) in rapamycin-treated animals compared with vehicle-treated controls. Levels of cyclin D1, proliferating cell nuclear antigen, and Ki-67 were also decreased in BCCs harvested from UV-irradiated/rapamycin-treated Ptch1$^{+/-}$ mice (Figure 5f and g). In addition, the tumor-adjacent skin of the rapamycin-treated animals showed

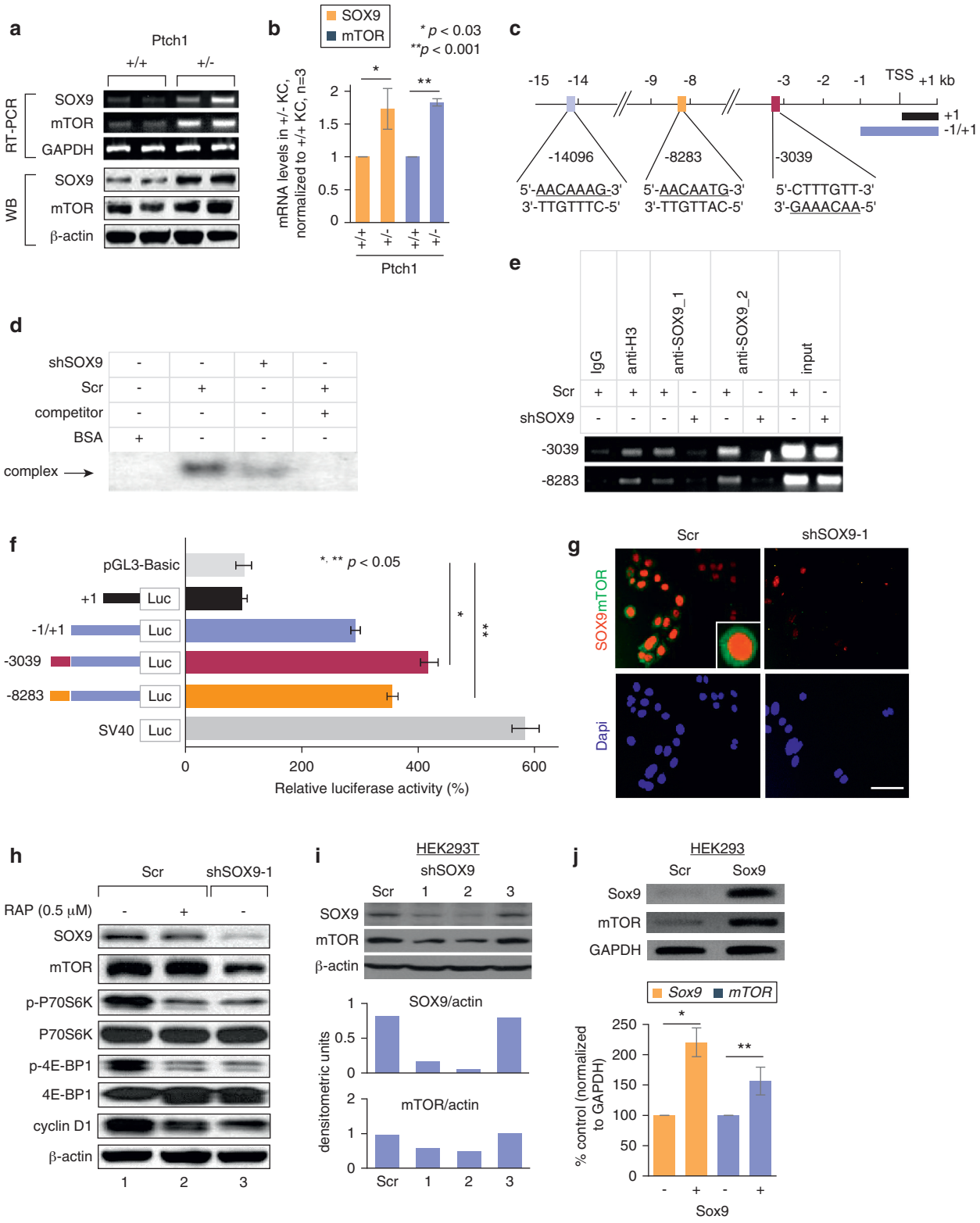

Figure 3. SOX9 transcriptionally regulates mTOR. SOX9 and mTOR levels in primary keratinocytes isolated from postnatal day 2 Ptch1$^{+/-}$ (+/−) and wild-type Ptch1$^{+/+}$ (+/+) mice, assessed by (**a**)western blotting and RT-PCR and (**b**) quantitative RT-PCR. Quantitative RT-PCR data represent the mean ± SD of three independent experiments. *$P < 0.03$, **$P < 0.001$ (+/+ vs. +/−). (**c**) Consensus SOX9 motifs in the mouse *Mtor* promoter. (**d**) Electrophoretic mobility shift assay to assess binding at −3039 in ASZ001 cells transduced with Scr or shSOX9-1. (**e**) Chromatin immunoprecipitation studies of SOX9 (anti-SOX9_1, anti-SOX9_2) binding to the *Mtor* promoter. (**f**) mTOR promoter-driven luciferase activities in the presence or absence of SOX9 motifs in ASZ001 cells. Data represent the mean ± SD of three independent experiments. (**g**) Immunofluorescent detection of SOX9 and mTOR in ASZ001 cells transduced with shScr or shSOX9-1. Scale bar = 100 μm. (**h**) SOX9 knockdown attenuates mTOR signaling in ASZ001 cells, comparable to that treated with rapamycin, assessed by

increased expression of the apoptotic proteins, Bax, and cleaved caspase-3 and showed a concurrent decrease in antiapoptotic Bcl2 levels (Figure 5h). Our data demonstrate the preclinical efficacy of rapamycin and confirm the importance of mTOR as a potential alternative target in UV-induced BCC tumorigenesis in Ptch1$^{+/-}$ mice.

DISCUSSION

SOX9 belongs to group E of the SOX transcription factor family (SOX8, SOX9, and SOX10), which is defined by a common high mobility group box domain originally identified in SRY, the sex-determining gene on the Y chromosome (Lefebvre et al., 2007). SOX9 is crucial during fetal development, and germline SOX9 mutations cause skeletal malformations, central nervous system dysfunction, and multiple defects in additional organs. SOX9 also contributes to the maintenance of stem/progenitor cells in the liver, pancreas, and hair follicles (Furuyama et al., 2011; Vidal et al., 2005). Consequently, dysregulated SOX9 expression has been linked to the initiation and growth of a wide range of tumors: it has been shown to enhance proliferation and migration of prostate cancer cells and the formation of pancreatic ductal adenocarcinomas and is also implicated in metastasis and endocrine resistance in breast cancer (Deng et al., 2015; Jeselsohn et al., 2017). In murine BCCs, SOX9 was recently shown to be required for tumor initiation in a Wnt/β-catenin-dependent manner (Larsimont et al., 2015). Moreover, cooperative Hh-EGFR signaling promotes synergistic induction of SOX9 in Hh-driven BCCs (Eberl et al., 2012). These results suggest that Hh signaling can be modulated at multiple levels, and that downstream mediators of SOX9 likely play an important regulatory role in BCC growth.

In that regard, our study has identified mTOR as a transcriptional target of SOX9. We show that consensus SOX9-binding motifs exist in the mTOR promoter, and that SOX9 occupies these sites and induces mTOR transcriptional activity in ASZ001 cells. Furthermore, attenuated mTOR expression and mTOR-dependent growth signaling in SOX9 knockdown ASZ001 cells validate the importance of the SOX9-mTOR axis in BCC growth. In support of its oncogenic role in BCC, SOX9 deletion was recently shown to prevent SMO-driven BCC formation in K14CreER:SmoM2 mice (Larsimont et al., 2015). In this study, SOX9 was shown to regulate many cancer-specific genes, including those that promote stemness, extracellular matrix deposition, and cytoskeleton remodeling while repressing epidermal differentiation, adding complexity to the transcriptional network underlying BCC growth. Given the difference between their K14CreER:SmoM2 model that carries an activating SMO mutant and our in vitro and in vivo models that reflect UV-induced BCC carcinogenesis, it would be interesting to determine the status of SOX9 regulatory networks in these models. Interestingly, our analysis of their chromatin immunoprecipitation-seq data revealed the presence of several SOX9 binding regions in the mTOR promoter, and similar to our findings, these regions were located distant from the TSS (Larsimont et al., 2015). Although further investigation is warranted for clarifying the functional relevance of these regions, a large fraction of SOX9 bound regions in chondrocytes are localized at a considerable distance from the TSS (Ohba et al., 2015). In fact, direct DNA binding through dimeric SOX9 recognition within evolutionarily conserved enhancer elements extends tens to hundreds of kilobases from the TSS of the target gene (Ohba et al., 2015). Moreover, SOX9 association with the TSS domain has been shown to engage basal activities in chondrocytes and likely occurs via protein-protein interactions with the basal transcription apparatus (Ohba et al., 2015). Although this may argue for the substantial reporter activities that we observed with the −1 kb region of the mTOR promoter that lacks apparent SOX9-binding motifs, we cannot completely exclude the possibility that SOX9-independent mechanisms can regulate mTOR. In fact, multiple transcriptional factors (e.g., NRF2, AP-1) and pathways (e.g., WNT, RAS, p53) are known to regulate mTOR (Bendavit et al., 2016; Chiarini et al., 2015; Saxton and Sabatini, 2017). Their relevance to mTOR signaling and BCC pathogenesis remains to be elucidated.

Up to now, the studies exploring the role of mTOR in BCCs have been largely limited to immunohistochemical assessment. These studies show variable degrees of mTOR or p-mTOR staining in BCCs that ranges from 8% to 18% (Brinkhuizen et al., 2014; Gutierrez-Dalmau et al., 2010; Karayannopoulou et al., 2013). In contrast, our study demonstrates that mTOR is overexpressed in a substantial fraction of human BCCs (56%, n = 50). This variable immunoreactivity may be due in part to the use of different antibodies and staining protocols, as well as to differential antibody specificities. Nevertheless, the substantial reduction in BCC growth observed in our study in rapamycin-treated Ptch1$^{+/-}$/SKH-1 mice underscores the importance of mTOR signaling in BCC tumorigenesis. In support of our data, partial to complete BCC regression, albeit with a limited sample size (n = 4), was recently reported in patients treated with everolimus, a derivative of rapamycin (1.5–3 mg daily for 12 months or longer) (Eibenschutz et al., 2013). The combined treatment of sonidegib and the phosphatidylinositol 3/mTOR dual inhibitor, dactolisib, was also shown to suppress the emergence of SMO resistance in a medulloblastoma xenograft model, further supporting the relevance of the phosphatidylinositol 3-mTOR pathway in Hh-dependent tumors (Buonamici et al., 2010). Aberrant mTOR signaling has also been implicated in SCC development (Balagula et al., 2015). Although our study, demonstrating the preclinical efficacy of rapamycin against UV-induced SCCs in Ptch1$^{+/-}$/SKH-1 mice, confirms the importance of mTOR signaling in SCC growth, it is of interest that SOX9 was largely absent in both murine and human SCCs, excluding the possibility of SOX9

western blotting. (**i**) mTOR levels in SOX9 knockdown HEK293T cells, detected by western blotting. Histogram: densitometric scanning of western blots, normalized to actin. (**j**) mTOR expression in SOX9-overexpressing HEK293 cells, assessed by RT-PCR. Histogram: data represent the mean ± SD of two independent experiments. *$P = 0.044$, **$P = 0.037$. 4E-BP1, 4E binding protein 1; GAPDH, glyceraldehyde-3-phosphate dehydrogenase; GLI, glioma-associated oncogene homolog; HEK, human embryonic kidney; mTOR, mammalian target of rapamycin; PTCH1, patched 1; RT-PCR, reverse transcriptase-PCR; SD, standard deviation; SOX9, Sry-related high mobility group box 9; TSS, transcription start site.

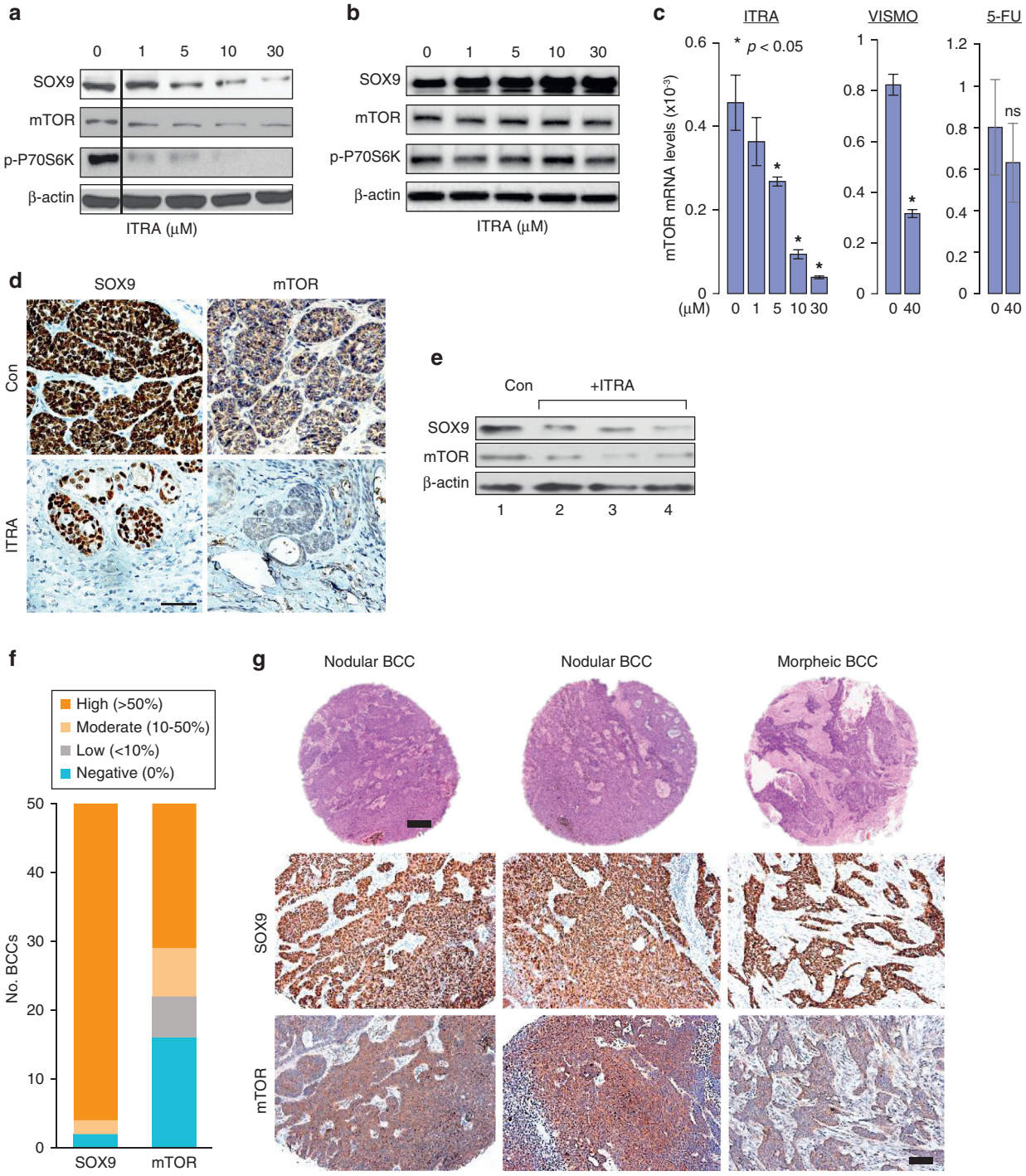

Figure 4. Hedgehog signaling regulates mTOR via SOX9. Levels of SOX9, mTOR, and p-p70S6K in (**a**) ASZ001 cells or in (**b**) ASZ001 cells overexpressing SOX9 treated with varying concentrations of ITRA for 24 hours, assessed by western blotting. (**c**) Quantitative RT-PCR analysis for mTOR levels in ASZ001 cells treated with ITRA, VISMO, or 5-FU. Data represent the mean ± SD of three independent experiments. *$P < 0.05$, compared with nontreated controls; ns, statistically not significant. (**d, e**) SOX9 and mTOR levels in UV-induced BCCs treated with ITRA or vehicle (Con) in Ptch1$^{+/-}$ mice. Representative immunohistochemical images (**d**), and western blotting analysis of extracts prepared from BCC lesions excised from different mice (lanes 1−4) (**e**). Scale bar = 50 μm. (**f, g**) SOX9 and mTOR levels in human BCCs, assessed by immunohistochemical analysis of human BCC tissue microarray (n = 50). Histogram bars represent the number of BCCs corresponding to the percentage of positively stained tumor cells within the tumor areas (**f**); representative hematoxylin and eosin and immunohistochemical images of nodular and morpheic BCCs (**g**). Scale bars = 50 μm. 5-FU, 5-fluorouracil; BCC, basal cell carcinoma; ITRA, itraconazole; mTOR, mammalian target of rapamycin; PTCH1, patched 1; RT-PCR, reverse transcriptase PCR; SD, standard deviation; SOX9, Sry-related high mobility group box 9; VISMO, vismodegib.

regulation of mTOR in SCC. It is also worth pointing out that although SOX9 expression was observed in the majority of BCC cells, not all SOX9-positive BCC cells expressed mTOR at a level detectable by immunohistochemistry, suggesting that the SOX9-mTOR axis may be operable in subpopulations of BCCs. In summary, our study, demonstrating the

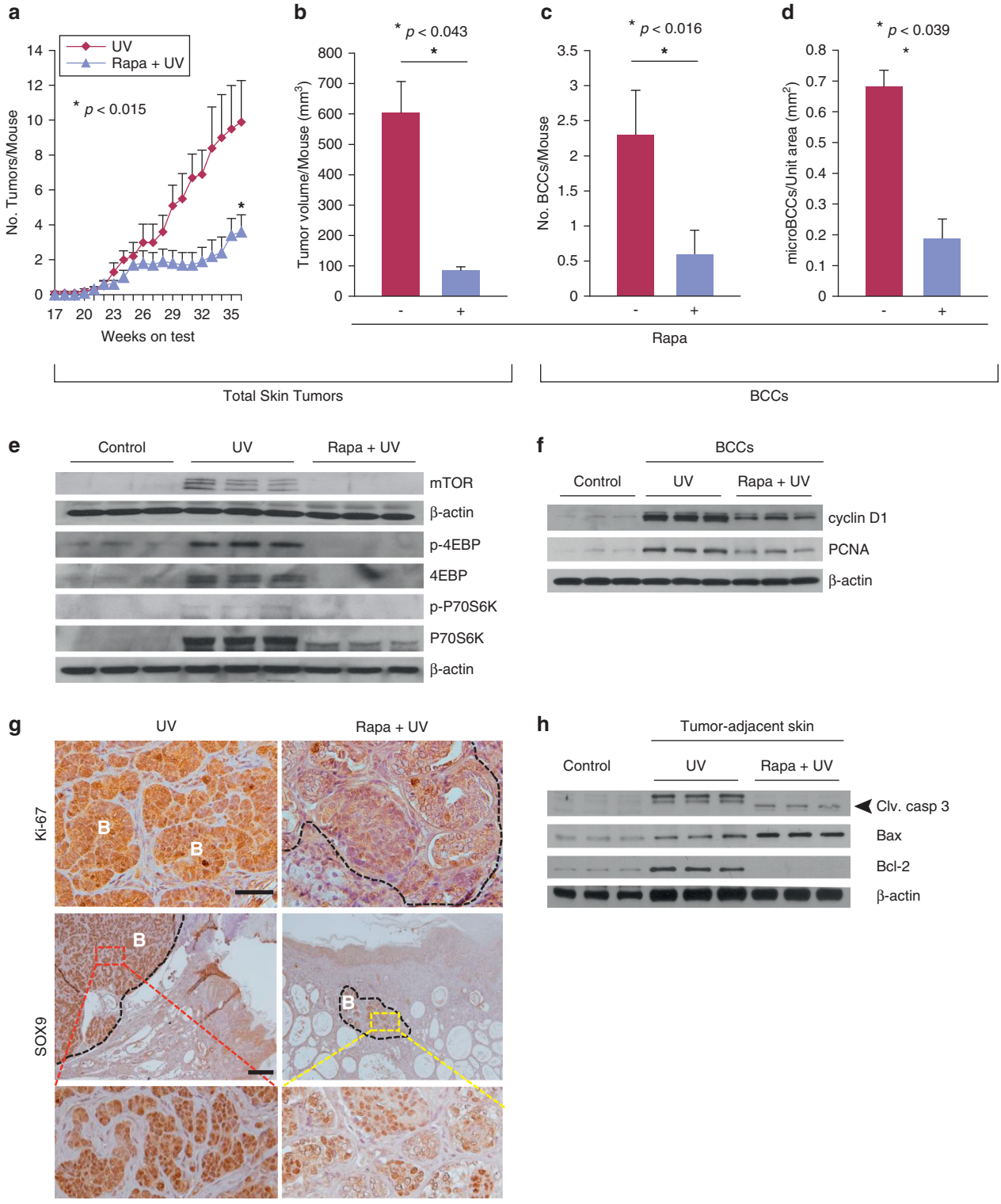

Figure 5. Rapamycin decreases mTOR levels and suppresses UV-induced growth of BCC in Ptch1$^{+/-}$ mice. The total (**a**) number and (**b**) volume of UV-induced skin tumors are significantly reduced in mice treated with rapamycin (40 μg/mouse, intraperitoneal) for 36 weeks. Decreases in (**c**) visible and (**d**) microscopic BCC burden in rapamycin-treated mice. Data represent the mean ± standard error of the mean. *$P < 0.05$ compared with nontreated mice at week 36. Decreases in mTOR levels and phosphorylations of mTOR substrates (**e**), and cell cycle progression and proliferation markers cyclin D1 and PCNA (**f**) in rapamycin-treated mice, as assessed by western blotting. (**g**) Immunohistochemical distribution of Ki-67 and SOX9 in BCCs from rapamycin- and vehicle-treated mice. B, BCC. (**h**) The effects of rapamycin on apoptosis markers, cleaved caspase-3, Bax, and Bcl2, in tumor-adjacent Ptch1$^{+/-}$ skin. Western blotting. Control, age-matched, nonirradiated skin. 4E-BP, 4E binding protein; BCC, basal cell carcinoma; mTOR, mammalian target of rapamycin; PCNA, proliferating cell nuclear antigen; PTCH1, patched 1; SOX9, Sry-related high mobility group box 9.

convergence of Hh signaling on mTOR and the preclinical efficacy of targeting mTOR, could provide additional strategies to enhance the therapeutic ratio associated with SMO inhibitor therapy in patients with BCNS. Further investigation of the SOX9 regulatory network may also reveal as yet undefined molecular processes governing BCC pathogenesis and in turn may reveal additional mechanism-driven targets for the chemoprevention and treatment of this most common type of human malignancy.

MATERIALS AND METHODS

Cells and reagents

ASZ001 cells (a gift from Dr Ervin Epstein) were cultured as previously described (So et al., 2006). HEK293 and HEK293T cells were cultured in DMEM supplemented with 10% fetal bovine serum. Vismodegib and 5-fluorouracil were purchased from Selleckchem (Houston, TX); ITRA was from Sigma-Aldrich (St. Louis, MO) and SPORANOX 100 mg/10 ml from Janssen Pharmaceuticals (Titusville, NJ). Antibodies against mTOR, p-p70S6K, p70S5K, p-4E-BP1, 4E-BP1, and p-AKT were from Cell Signaling Technology (Danvers, MA); cyclin D1, cleaved caspase-3, Bax, and Bcl-2 from Santa Cruz Biotechnology (Santa Cruz, CA); SOX9 and proliferating cell nuclear antigen from Abcam (Cambridge, MA); and β-actin from Sigma-Aldrich.

Western blot analysis, immunohistochemistry, and immunofluorescence

Experiments were performed as previously described (Kim et al., 2002a, 2002b, 2016). Western blotting analysis of human BCCs utilized surgically excised human BCC specimens (n = 6) obtained from the Dermatologic Surgery Unit of the Department of Dermatology, in compliance with the Columbia University Medical Center IRB exemption (IRB-AAAB1948). Tissue samples were not associated with patient names, hospital numbers, or other identifying information, other than the patient's age, anatomical location, and diagnosis. Quantitation of band intensities was performed with the ImageJ software (http://imagej.nih.gov/ij/).

Tissue microarrays

Human BCC tissue microarrays (SK-803a, US Biomax, Rockville, MD) and human SCC tissue microarrays (IMH-323, Novus Biologicals, Littleton CO)—representing a total of 50 BCCs and 32 SCCs, respectively—were used in the immunohistochemical assessment of mTOR and SOX9. The human SCC tissue arrays included two invasive SCCs and two recurrent SCCs. Tissue sections were treated with antigen unmasking solution (Vector Labs, Burlingame, CA) before incubation with primary antibodies and visualized with 3,3-diaminobenzidine, as previously described (Kim et al. 2016; Liu et al., 2014). Positive staining for SOX9 and mTOR was defined as nuclear or cytoplasmic staining of a tumor cell, respectively. Scores were assigned using a 0−3 scale to denote the prevalence of positive cells within tumor areas, where 0 = negative (0%), 1 = low (<10%), 2 = moderate (10%−50%), and 3 = high (>50%). Because SOX9 staining was barely detectable in the majority of SCCs examined in this study, scores >1 were considered positive.

SOX9 knockdown and overexpression

shRNA constructs that target both mouse and human *SOX9* (29mer shRNA constructs in lentiviral GFP vector [Locus ID 6662]) and scrambled control shRNA were purchased from OriGene (Rockville, MD). Transduction and generation of stable *SOX9* knockdown ASZ001 and HEK293T cell lines were performed using shSOX9-1 (TGCATCCGCGAGGCGGTCAGCCAGGTGCT), shSOX9-2 (GTGCGCGTCAACGGCTCCAGCAAGAACAA), and shSOX9-3 (CAGCGAACGCACATCAAGACGGAGCAGCT), according to the guidelines of the Phoenix Retroviral Expression System (Orbigen, San Diego, CA). Mouse myc-tagged *Sox9* construct (OriGene, Rockville, MD) was transiently transfected into HEK293 cells according to the manufacturer's instructions.

5-Ethynyl-2′-deoxyuridine incorporation assay

The proliferative capacity of SOX9 knockdown ASZ001 cells was assessed using a Click-iT Plus 5-ethynyl-2′-deoxyuridine Alexa Fluor 488 Imaging Kit (Thermo Fisher, Waltham, MA). For labeling, 5-ethynyl-2′-deoxyuridine was added directly to the cell culture, to a final concentration of 10 μM; cultures were incubated for 2 hours, at which point cells were fixed, permeabilized, and labeled with Alexa Fluor picolyl azidea, according to the manufacturer's instructions.

Animal study

The Institutional Animal Care and Use Committee of the University of Alabama at Birmingham approved the animal studies. Six- to eight-week-old Ptch1$^{+/-}$ mice were divided into three groups of 20 each. Group I animals served as an age-matched vehicle control (negative control). Group II and group III animals were irradiated with UV (180 mJ/cm^2; twice/week) for 36 weeks. In addition, 60 minutes before UV irradiation, group II received a vehicle (phosphate buffered saline) and group III received intraperitoneal injections of rapamycin (40 μg/mouse in 100 μl phosphate buffered saline). Rapamycin stock (50 mg/ml) was prepared in Cremophor EL and ethanol. The number and sizes of tumors were recorded weekly using an electronic Vernier Caliper, as previously described (Chaudhary et al., 2015). After 36 weeks, skin and tumor tissues were harvested and processed for histological and biochemical analysis. The ITRA study protocol was previously described (Kim et al., 2016).

Statistical analyses

Statistical analyses were performed using Student's *t* test (two-tailed): $P < 0.05$ was considered statistically significant.

Additional methods are provided in the Supplementary Materials online.

CONFLICT OF INTEREST

The authors state no conflict of interest.

ACKNOWLEDGMENTS

This work was partially supported by Irving Scholar Award (ALK), and the NIH Grants (R01ES020344 to DRB, and R01ES026219 to MA).

SUPPLEMENTARY MATERIAL

Supplementary material is linked to the online version of the paper at www.jidonline.org, and at https://doi.org/10.1016/j.jid.2018.01.040.

REFERENCES

Aszterbaum M, Rothman A, Johnson RL, Fisher M, Xie J, Bonifas JM, et al. Identification of mutations in the human PATCHED gene in sporadic basal cell carcinomas and in patients with the basal cell nevus syndrome. J Invest Dermatol 1998;110:885−8.

Athar M, Li C, Kim AL, Spiegelman VS, Bickers DR. Sonic hedgehog signaling in basal cell nevus syndrome. Cancer Res 2014;74:4967−75.

Atwood SX, Chang AL, Oro AE. Hedgehog pathway inhibition and the race against tumor evolution. J Cell Biol 2012;199:193−7.

Atwood SX, Sarin KY, Whitson RJ, Li JR, Kim G, Rezaee M, et al. Smoothened variants explain the majority of drug resistance in basal cell carcinoma. Cancer Cell 2015;27:342−53.

Balagula Y, Kang S, Patel MJ. Synergism between mTOR pathway and ultraviolet radiation in the pathogenesis of squamous cell carcinoma and its

implication for solid-organ transplant recipients. Photodermatol Photoimmunol Photomed 2015;31:15–25.

Bendavit G, Aboulkassim T, Hilmi K, Shah S, Batist G. Nrf2 transcription factor can directly regulate mTOR: linking cytoprotective gene expression to a major metabolic regulator that generates redox activity. J Biol Chem 2016;291:25476–88.

Bien-Willner GA, Stankiewicz P, Lupski JR. SOX9cre1, a cis-acting regulatory element located 1.1 Mb upstream of SOX9, mediates its enhancement through the SHH pathway. Hum Mol Genet 2007;16:1143–56.

Brinkhuizen T, Weijzen CAH, Eben J, Thissen MR, van Marion AM, Lohman BG, et al. Immunohistochemical analysis of the mechanistic target of rapamycin and hypoxia signalling pathways in basal cell carcinoma and trichoepithelioma. PLoS One 2014;9:e106427.

Briscoe J, Therond PP. The mechanisms of Hedgehog signalling and its roles in development and disease. Nat Rev Mol Cell Biol 2013;14:416–29.

Buonamici S, Williams J, Morrissey M, Wang A, Guo R, Vattay A, et al. Interfering with resistance to smoothened antagonists by inhibition of the PI3K pathway in medulloblastoma. Sci Transl Med 2010;2:51ra70.

Chaudhary SC, Tang X, Arumugam A, Li C, Srivastava RK, Weng Z, et al. Shh and p50/Bcl3 signaling crosstalk drives pathogenesis of BCCs in gorlin syndrome. Oncotarget 2015;6:36789–814.

Chiarini F, Evangelisti C, McCubrey JA, Martelli AM. Current treatment strategies for inhibiting mTOR in cancer. Trends Pharmacol Sci 2015;36:124–35.

Deng W, Vanderbilt DB, Lin C-C, Martin KH, Brundage KM, Ruppert JM. SOX9 inhibits β-TrCP-mediated protein degradation to promote nuclear GLI1 expression and cancer stem cell properties. J Cell Sci 2015;128:1123–38.

Eberl M, Klingler S, Mangelberger D, Loipetzberger A, Damhofer H, Zoidl K, et al. Hedgehog-EGFR cooperation response genes determine the oncogenic phenotype of basal cell carcinoma and tumour-initiating pancreatic cancer cells. EMBO Mol Med 2012;4:218–33.

Eibenschutz L, Colombo D, Catricalà C. Everolimus for compassionate use in multiple basal cell carcinomas. Case Rep Dermatol Med 2013;2013:604301.

Fonseca BD, Alain T, Finestone LK, Huang BPH, Rolfe M, Jiang T, et al. Pharmacological and genetic evaluation of proposed roles of mitogen-activated protein kinase/extracellular signal-regulated kinase kinase (MEK), extracellular signal-regulated kinase (ERK), and p90(RSK) in the control of mTORC1 protein signaling by phorbol esters. J Biol Chem 2011;286:27111–22.

Furuyama K, Kawaguchi Y, Akiyama H, Horiguchi M, Kodama S, Kuhara T, et al. Continuous cell supply from a Sox9-expressing progenitor zone in adult liver, exocrine pancreas and intestine. Nat Genet 2011;43:34–41.

Gorlin RJ. Nevoid basal-cell carcinoma syndrome. Medicine 1987;66:98–113.

Gutierrez-Dalmau A, Revuelta I, Ferrer B, Mascaro JM Jr, Oppenheimer F, Albanell J, et al. Distinct immunohistochemical phenotype of non-melanoma skin cancers between renal transplant and immunocompetent populations. Transplantation 2010;90:986–92.

Hahn H, Wicking C, Zaphiropoulous PG, Gailani MR, Shanley S, Chidambaram A, et al. Mutations of the human homolog of Drosophila patched in the nevoid basal cell carcinoma syndrome. Cell 1996;85:841–51.

Hui C-c, Angers S. Gli proteins in development and disease. Ann Rev Cell Dev Biol 2011;27:513–37.

Jeselsohn R, Cornwell M, Pun M, Buchwalter G, Nguyen M, Bango C, et al. Embryonic transcription factor SOX9 drives breast cancer endocrine resistance. Proc Natl Acad Sci USA 2017;114:E4482–91.

Johnson RL, Rothman AL, Xie J, Goodrich LV, Bare JW, Bonifas JM, et al. Human homolog of patched, a candidate gene for the basal cell nevus syndrome. Science 1996;272:1668–71.

Kadaja M, Keyes BE, Lin M, Pasolli HA, Genander M, Polak L, et al. SOX9: a stem cell transcriptional regulator of secreted niche signaling factors. Genes Dev 2014;28:328–41.

Kar S, Deb M, Sengupta D, Shilpi A, Bhutia SK, Patra SK. Intricacies of hedgehog signaling pathways: a perspective in tumorigenesis. Exp Cell Res 2012;318:1959–72.

Karayannopoulou G, Euvrard S, Kanitakis J. Differential expression of p-mTOR in cutaneous basal and squamous cell carcinomas likely explains their different response to mTOR inhibitors in organ-transplant recipients. Anticancer Res 2013;33:3711–4.

Kim A, Back J, Zhu Y, Tang X, Yardley N, Athar M, et al. Akt1 activation is obligatory for spontaneous BCC tumor growth in a murine model that mimics some features of basal cell nevus syndrome. Cancer Prev Res 2016;9:794–802.

Kim AL, Athar M, Bickers DR, Gautier J. Stage-specific alterations of cyclin expression during UVB-induced murine skin tumor development. Photochem Photobiol 2002a;75:58–67.

Kim AL, Athar M, Bickers DR, Gautier J. Ultraviolet-B-induced G1 arrest is mediated by downregulation of cyclin-dependent kinase 4 in transformed keratinocytes lacking functional p53. J Invest Dermatol 2002b;118:818–24.

Kim AL, Back JH, Zhu Y, Tang X, Yardley NP, Kim KJ, et al. AKT1 activation is obligatory for spontaneous BCC tumor growth in a murine model that mimics some features of basal cell nevus syndrome. Cancer Prev Res 2016;9:794.

Kim J, Tang JY, Gong R, Kim J, Lee JJ, Clemons KV, et al. Itraconazole, a commonly used antifungal that inhibits Hedgehog pathway activity and cancer growth. Cancer Cell 2010;17:388–99.

Kinzler KW, Vogelstein B. The GLI gene encodes a nuclear protein which binds specific sequences in the human genome. Mol Cell Biol 1990;10:634–42.

Larsimont J-C, Youssef Khalil K, Sánchez-Danés A, Sukumaran V, Defrance M, Delatte B, et al. Sox9 controls self-renewal of oncogene targeted cells and links tumor initiation and invasion. Cell Stem Cell 2015;17:60–73.

Lefebvre V, Dumitriu B, Penzo-Méndez A, Han Y, Pallavi B. Control of cell fate and differentiation by Sry-related high-mobility-group box (Sox) transcription factors. Int J Biochem Cell Biol 2007;39:2195–214.

Liu L, Rezvani HR, Back JH, Hosseini M, Tang X, Zhu Y, et al. Inhibition of p38 MAPK signaling augments skin tumorigenesis via NOX2 driven ROS generation. PLoS One 2014;9:e97245.

Ohba S, He X, Hojo H, McMahon AP. Distinct transcriptional programs underlie Sox9 regulation of the mammalian chondrocyte. Cell Rep 2015;12:229–43.

Pricl S, Cortelazzi B, Dal Col V, Marson D, Laurini E, Fermeglia M, et al. Smoothened (SMO) receptor mutations dictate resistance to vismodegib in basal cell carcinoma. Mol Oncol 2015;9:389–97.

Robbins DJ, Fei DL, Riobo NA. The Hedgehog signal transduction network. Sci Signal 2012;5:re6.

Saxton RA, Sabatini DM. mTOR signaling in growth, metabolism, and disease. Cell 2017;168:960–76.

Sharpe HJ, Pau G, Dijkgraaf GJ, Basset-Seguin N, Modrusan Z, Januario T, et al. Genomic analysis of smoothened inhibitor resistance in basal cell carcinoma. Cancer Cell 2015;27:327–41.

So PL, Langston AW, Daniallinia N, Hebert JL, Fujimoto MA, Khaimskiy Y, et al. Long-term establishment, characterization and manipulation of cell lines from mouse basal cell carcinoma tumors. Exp Dermatol 2006;15:742–50.

Tang JY, Mackay-Wiggan JM, Aszterbaum M, Yauch RL, Lindgren J, Chang K, et al. Inhibiting the hedgehog pathway in patients with the basal-cell nevus syndrome. N Engl J Med 2012;366:2180–8.

Vidal VPI, Chaboissier M-C, Lützkendorf S, Cotsarelis G, Mill P, Hui C-C, et al. Sox9 is essential for outer root sheath differentiation and the formation of the hair stem cell compartment. Curr Biol 2005;15:1340–51.

Vidal VPI, Ortonne N, Schedl A. SOX9 expression is a general marker of basal cell carcinoma and adnexal-related neoplasms. J Cutan Pathol 2008;35:373–9.